Understanding Drought Awareness from Web Data

Mashrekur Rahman[a], Samuel Sandoval Solis[b], Thomas Harter[c], Mahmoud Saeedimoghaddam[d], Niv Efron[e], Grey S. Nearing[f]

[a]*Department of Land, Air and Water Resources, University of California, Davis, One Shields Avenue, Davis, 95616, CA, USA*
[b]*Department of Land, Air and Water Resources, University of California, Davis, One Shields Avenue, Davis, 95616, CA, USA*
[c]*Department of Land, Air and Water Resources, University of California, Davis, One Shields Avenue, Davis, 95616, CA, USA*
[d]*Department of Land, Air and Water Resources, University of California, Davis, One Shields Avenue, Davis, 95616, CA, USA*
[e]*Google Research, 1600 Amphitheatre Parkway, Mountain View, 94043, CA, USA*
[f]*Google Research, 1600 Amphitheatre Parkway, Mountain View, 94043, CA, USA*

Abstract

We used computer vision (U-Net) model to leverage Standardized Precipitation Evapotranspiration Index (SPEI), Google Trends Search Interest (SI), and Twitter data to understand patterns with which people in Continental United States (CONUS) indicate awareness of and interest in droughts. We found significant statistical relationships between the occurrence of meteorological droughts (MD), as measured by SPEI, and SI on drought topics over CONUS. SI tends to lag MD by a period of 2-3 months, however relationships between MD and corresponding SI varies significantly over the CONUS in both space and time. People in states with increasingly dry conditions have become increasingly interested in drought topics. However, with worsening drought conditions in California, public SI on drought topics in the state has not increased significantly between 2016 and 2020, despite the overall SI

being high. We additionally applied sentiment analysis on 5 million tweets related to droughts and found that public emotions towards drought have become more polarized.

1. Introduction

Economic damage caused by droughts in the United States is estimated to be in the billions of dollars [1]. Public perceptions and attitudes towards droughts – both pre- and post-drought – are indicators of public reception of water management and conservation measures [2, 3]. Adams et al. [4] assessed the influence of attitudes and perceptions regarding multiple factors on water conservation use in nine U.S. states and found that public perception of the importance of water resources management significantly influenced water conservation outcomes. A study on the sociological impacts of drought perception in South-Central Nebraska revealed that crop and livestock producers were becoming increasingly concerned about water scarcity resulting from droughts [5]. Similar concerns were shared by farmers in a study conducted in the Jucar River Basin in Spain [6] and in South Africa [7]. After a record breaking drought in Texas in 2011, residents were significantly more concerned with water availability and water conservation [8]. A recent study on two cities in Alabama found that public awareness of drought is significantly dependent on geographic, physical, and social contexts [9]. They used

2

Google Trends data in addition to survey data and suggested that future studies consider Twitter data to gain a more complete understanding of social responses to drought hazards. However, a Continental United States (CONUS)-scale study of human-drought interactions using web data has not been conducted.

Evaluating public responses based upon questionnaire surveys is expensive, time consuming, and often constrained by small sample-sizes [10, 11]. In addition, questionnaire responses can be hard to interpret because of social context, such as, non-response or social-desirability biases [12, 13]. The rise of internet use means that a wide array of data sources have become available to researchers. Search trends and social media data, although not without their own limitations, can help mitigate some of the issues with direct surveys. Internet users encompass most demographics and social-economic groups from large geographic ranges. In 2018, 92% of households in the United States had at least one type of computer and 85% had a broadband internet subscription [14]. This makes a geographical area such as the CONUS an ideal candidate for a large-scale web-based study. Numerous previous studies (some examples mentioned below) have used internet query data as a proxy for survey data in a diverse range of research topics. Carneiro et al. [15] argued that Google Trends Search Interest (SI) data has the potential to track disease activity and outbreaks earlier than traditional surveillance systems. Yang et al. [16] successfully used Google Insights, which provides time series data of weekly search trends data, as a proxy for surveys to investigate large-scale seasonal

3

patterns of depression. Stephens-Davidowitz [17] argued that using Google search interest data as a proxy for racial animus provides a more substantial estimate of its impact on electoral outcomes compared to survey-based approaches. Hong et al. [18] used internet search volume data from Google Trends as a proxy for population interest in telehealth and telemedicine, and Arora et al. [19] comprehensively discussed the versatility and potential of using Google search engine data as a proxy for survey in population health research. Mellon [20] emphasized that in addition to its obvious advantages with spatial coverage, Google search data can also provide more frequent and timely information compared to surveys, as search trends are measured on a weekly basis, allowing for easier comparisons over time. Given the broad use of SI data as proxies for survey data, we utilize SI as a proxy for people's awareness of and interest in Meteorological Droughts (MD).

1.1. Research Questions

In this paper, we address the following research questions:

- Do people respond to meteorological droughts by searching drought terms on Google and is there a time lag between occurrence of meteorological droughts and rise in people's search interest in droughts?

- Does the relationship between MD occurrences and people's SI exhibit spatial variation across CONUS?

- Have people in meteorological drought hotspots become increasingly interested in drought topics?

4

- How have people's sentiments about drought changed over time?

Understanding the public's responses and sentiment towards meteorological droughts offers key insights for decision makers who can leverage these insights for early warnings, public service announcements, or targeted water conservation initiatives. Recognizing shifts in sentiments aids in tailoring effective messaging to communities. Such insights directly align with societal objectives, notably, reducing water consumption.

2. Methods

In this section, we discuss the data-driven experimental approaches and methods that we used to address the research questions outlined above.

To address the first research question, we first looked at variations in SI across CONUS within a study period (2004-2020). We then explored (non-linear) correlations between the occurrences of MD and people's search interest in drought topics. We investigated whether there is a temporal lag between MD indices and a subsequent rise in SI. We addressed these questions by using a machine learning models (trained on lagged data) to help uncover nonlinear correlations at various temporal lags.

To answer the second research question, we tested for spatial variability in statistical relationships between MD and public SI across CONUS. We explored this variability at a state-level.

For the third research question, we analyzed whether public SI in drought topics has increased in regions frequently affected by MD. We first observed

5

Table 1: Overview of data sources and availability

Data	Abbreviation	Source	Years Available	Years Used
Standardized Precipitation and Evapotranspiration Index	SPEI	spei.csic.es	1900-2020	2004-2020
Google Trends Search Interest	SI	Google Trends API (trends.google.com)	2004-Present	2004-2020
Tweets	NA	Twitter API (developer.twitter.com/en/docs/twitter-api)	2006-Present	2008-2020

distributions and trends of MD and subsequent public SI across CONUS and within individual states for our study period. We broke down this analysis into smaller time periods to look at drought hotspots and trends over shorter time spans.

To address the fourth research question, we leveraged a data set of five million tweets containing drought-related terms, with the aim of tracking changing sentiments towards drought over time. We achieved this by measuring the percentage of sentiments in people's tweets about drought terms between 2008 and 2020.

2.1. Data

Table 1 summarizes the three data types used in this study, including where the data was sourced and the temporal periods that we acquired and used.

2.1.1. Standardized Precipitation and Evapotranspiration Index (SPEI)

We acquired meteorological drought data from 1900 to 2020 from the Standardized Precipitation and Evapotranspiration Index (SPEI) data set [21]. SPEI is calculated by taking the difference between total precipitation and total potential evapotranspiration (PET) over a given period of time (e.g., monthly). SPEI is a standardized index, meaning that it is expressed

6

in units of standard deviations calculated over local (per pixel) climatologies, making it possible to compare drought conditions from different locations and different time periods. Calculating SPEI involves the following steps:

1. Calculate the difference between precipitation (P) and reference evapotranspiration ($ET0$) for each month or time step:

$$D_i = P_i - ET0_i \tag{1}$$

   where D_i is the difference between precipitation and reference evapotranspiration for the i-th month or time step, P_i is the precipitation for the i-th month or time step, and $ET0_i$ is the reference evapotranspiration for the i-th month or time step.

2. Calculate the climatic water balance for each month or time step:

$$WB_i = \sum_{j=1}^{n} D_{i-j+1} \tag{2}$$

   where WB_i is the climatic water balance for the i-th month or time step, and n is the time scale (e.g., 3, 6, or 12 months).

3. Fit a probability distribution, such as the three-parameter log-logistic distribution with the Maximum Likelihood Estimation (MLE) method, to the climatic water balance values:

$$F(WB) = \frac{1}{1 + \left(\frac{WB-\alpha}{\beta}\right)^{-\gamma}} \tag{3}$$

where $F(WB)$ is the cumulative probability distribution of the climatic water balance, and α, β, and γ are the distribution parameters that need to be estimated.

4. Calculate SPEI by transforming the fitted probability distribution to a standard normal distribution:

$$SPEI = \Phi^{-1}(F(WB)) \tag{4}$$

where SPEI is the Standardized Precipitation Evapotranspiration Index, Φ^{-1} is the inverse standard normal cumulative distribution function, and $F(WB)$ is the cumulative probability distribution of the climatic water balance.

SPEI can be calculated for a variety of time periods, ranging from 1 month to 48 months. We use monthly data in our calculations. Positive SPEI values indicate wetter conditions, while negative values indicate drier conditions. We created monthly SPEI maps over CONUS between 2004 and 2020. Fig 1 shows an example of one of these SPEI maps.

2.1.2. Google Trends Search Interest (SI)

We acquired Google Search Interest (SI) data from Google Trends using the Trends API. The Trends API allows programmatic access to Google trends data and track the popularity of different topics over time and place.

Given a specific term or topic, T, and a time range from t_1 to t_n, the search interest for T at each time point, t_i, is calculated as:
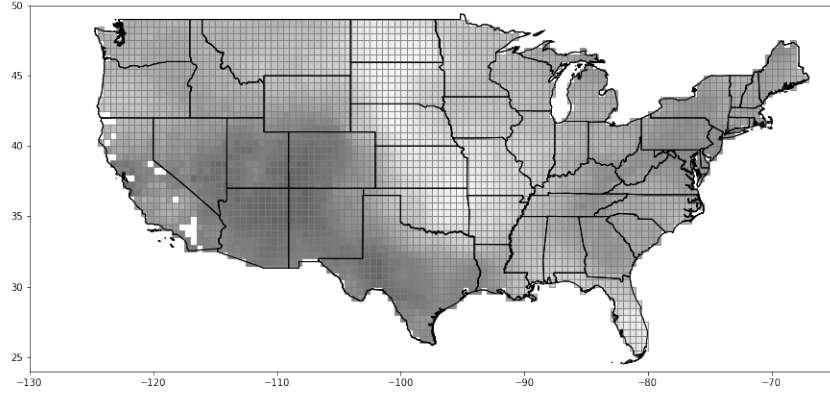
8

Figure 1: Example of a SPEI input map (Date: 08/16/2019). The image is in grayscale consistent with our actual input images.

$$SI(T, t_i) = \frac{S(T, t_i)}{S_{\max}(T)} \times 100 \tag{5}$$

where $SI(T, t_i)$ is the search interest for term or topic T at time point t_i, $S(T, t_i)$ is the search volume for T at t_i, and $S_{\max}(T)$ is the maximum search volume for T within the specified time range. We use monthly state-wise SI data on "Drought" topic from 2004 to 2020 to create maps over the CONUS. Fig 2 shows an example of a Google SI target map.

9
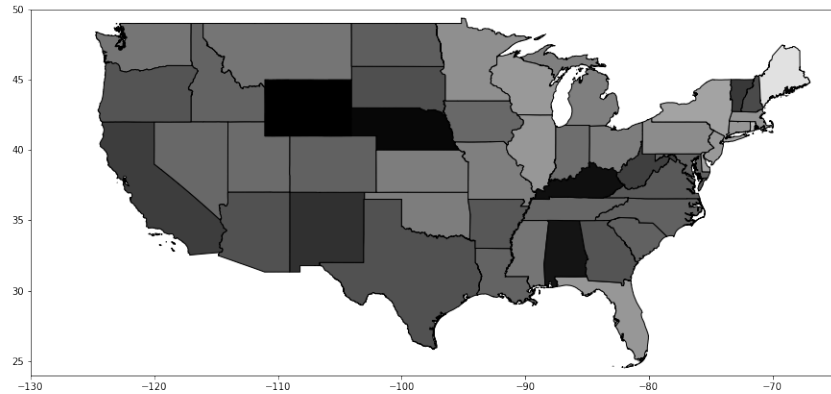
Figure 2: Example of a Google SI input map (Date: 08/2019). The image is in grayscale consistent with our actual target images into the model.

2.1.3. Tweets

We acquired Twitter data (Tweets) using the Twitter API. Our data set consists of 5 million tweets related to the "Drought" topic from 2008 to 2020. We use the Twitter data primarily for sentiment analysis. One thing to note is that Twitter data is not geotagged, so our only option is to use global tweets, but restricted to the English language.

2.2. Analysis Methods

2.2.1. SI analysis

To investigate how SI on droughts varies over CONUS, we first calculated the state-wise average SI on drought terms within the period of our study, and then rank states from highest to lowest values. We also calculated the overall change in average state-wise SI to reveal where SI has risen the most.

2.2.2. Relationship between MD and SI

We used machine learning models to estimate non-linear relationship(s) between MD and SI over CONUS. Specifically, we trained U-Net models [22] to predict SI from SPEI maps. Details of our model architecture, training, and evaluation are in Appendix Appendix A). In summary, we trained 6 models on 6 sets of lagged SPEI input maps (from 0 months lag to 5 months lag) and the target data were their corresponding SI maps. Correlation between (out-of-sample) SI predictions made by these trained models and real SI data is an estimate of the non-linear correlation between SPEI and SI at a given lag time. We evaluated the models on time periods not used for training (training period: 01/01/2004 - 07/31/2017 and test period: 08/01/2017 - 12/31/2020) and report their corresponding performances as correlation metrics.

2.2.3. Spatial variability of the relationship between MD and SI

We investigated spatial trends with respect to MD and corresponding public engagement in terms of SI. We first used trained U-Net models to pro-

duce outputs of time series of SI estimates during a test period (08/01/2017 to 12/31/2020) for each individual pixel in the SPEI maps:

$$O_{a,b}(t) = U(T_{a,b}(t)) \tag{6}$$

where $O_{a,b}(t)$ is the U-Net output for pixel (a, b) at time t, $T_{a,b}(t)$ is the input data for pixel (a, b) at time t, and U is the U-Net model function.

We then tested the model performance over time (using the coefficient of determination or R^2) for each individual pixel.

$$R_{a,b}^2 = R^2(O_{a,b}(t), G_{a,b}(t)) \tag{7}$$

where $R_{a,b}^2$ is the coefficient of determination for pixel (a, b), $G_{a,b}(t)$ is the ground truth (SI) data for pixel (a, b) at time t, and R^2 is the coefficient of determination function. We then created a binary mask array based on the geometry of CONUS and constructed heatmaps of the R^2 values. This approach allows us to observe overall model performances over time across CONUS, and also by individual states.

2.2.4. Best lag times per state

To investigate the existence of a temporal lag between occurrences of MD and rise in public SI on droughts, we found the time lag that gives the best SI predictions for each individual pixel. The different time lagged models are named $0ml$, $1ml$, $2ml$, $3ml$, $4ml$, and $5ml$. To perform this analysis, we

followed these steps:

First, we calculated the highest R^2 value for each model:

$$max\_r\_squared_{a,b} = \max_{k=1}^{6} R^2_{a,b,k} \tag{8}$$

where $max\_r\_squared_{a,b}$ is the highest R^2 value for pixel (a,b), and $R^2_{a,b,k}$ is the R^2 value for pixel (a,b) in model k.

Then we assigned each pixel with the highest R^2 value:

$$best\_model\_index_{a,b} = \arg\max_{k=1}^{6} R^2_{a,b,k} \tag{9}$$

where $best\_model\_index_{a,b}$ is the index of the model with the highest R^2 value for pixel (a,b). Looking at this map, we can assess the best lag times for each state.

2.2.5. Identifying MD hotspots over CONUS

We define MD hotspots as locations (SPEI pixels) that have been experiencing (on average) abnormally dry or drought conditions over the past 16 years (2004-2020). The reasoning behind choosing this time period is because (i) it is the length of the existing Google Trends data that we have available to apply our analyses on, and (ii) 16 years also encompasses a full cycle of wet and dry conditions. To identify meteorological drought hotspots, we performed the following steps:

We first calculated the average SPEI for the chosen period:

$$\overline{SPEI}_{a,b} = \frac{1}{N} \sum_{t=1}^{N} SPEI_{a,b}(t) \tag{10}$$

where $\overline{SPEI}_{a,b}$ is the average SPEI for pixel (a,b) over the whole study period (01/01/2004-12/31/2020), $SPEI_{a,b}(t)$ is the $SPEI$ value for pixel (a,b) at time t, and N is the total number of time steps within the chosen period (204 months).

In the next step, we normalize the $SPEI$ values:

$$SPEI'_{a,b} = \frac{\overline{SPEI}_{a,b} - \min(\overline{SPEI})}{\max(\overline{SPEI}) - \min(\overline{SPEI})} \tag{11}$$

where $SPEI'_{a,b}$ is the normalized $SPEI$ value for pixel (a,b), and $\min(\overline{SPEI})$ and $\max(\overline{SPEI})$ are the minimum and maximum average $SPEI$ values over CONUS, respectively. We generate a map of the meteorological drought distribution over CONUS and deem areas with average $SPEI$ below zero to be drought hotspots.

2.2.6. Exploring trends in MD hotspots

To understand whether people in meteorological drought hotspots have become increasingly interested in droughts, we conducted a state-wise trend analysis on both yearly SPEI and SI data for the full study period of 2004-2020 and also breaking the analysis period to 2004-2010, 2011-2015, and 2016-2020 to gain deeper insights into these trends. This involved fitting a linear regression model to the yearly SPEI and SI values for each state, and

14

extracting the slope of the fitted line as an indicator of the trend.

2.2.7. Sentiment analysis on Twitter data

We performed sentiment analysis on five million tweets related to drought topics. Sentiment analysis allows us to understand the tone of human generated texts. We used VADER (Valence Aware Dictionary and Sentiment Reasoner) – a lexicon and rule-based sentiment analysis tool that is specifically designed to work with social media data sets [23]. The overall sentiment score (compound score) assigned to a tweet is a number between -1 and 1. A score of -1 points towards a very negative sentiment while a score of 1 indicates a very positive sentiment. A neutral score of 0 indicates a neutral sentiment. We calculated the per-year percentages of these three sentiments within our tweet dataset and created a corresponding time series. Fig. 3 demonstrates an example of how a tweet about drought can receive a positive compound score (positive sentiment).

3. Results and Analysis

In this section we address the research questions laid out previously and discuss the results of our analyses.

15

	author id	created_at	geo	id	lang	like_count	quote_count	reply_count	retweet_count	source	tweet	sentiment
9	2768501	2008-01-03 07:04:19+00:00		557555292	en	0	0	0	0	Twitter Web Client	NFF welcomes talks with Govt on drought assist...	pos

Figure 3: Positive sentiment assigned to a tweet about drought

3.1. Do people respond to meteorological droughts by searching drought terms on Google and is there a time lag between occurrence of meteorological droughts and rise in people's search interest in drought?

The top 10 states by average SI over our study period were CA, NM, SD, CO, NE, WY, MT, ND, TX, and ID (Fig. 4). While the bottom 10 states were KY, LA, IL, TN, NJ, FL, OH, PA, NY, and MS. The top 10 states where people's yearly SI rose the most between years 2004 and 2020 were NH, ME, VT, CA, OR, RI, CT, DC, MA, and IA.

Average R^2 for the statistical relationship between pixel values of target images and predicted pixel values by the U-Net models are shown in Fig. 5. The U-Net's capacity for capturing nonlinear relationships is a key in this analysis. Results highlight significant nonlinear correlations between MD oc-

16

currences and associated anthropogenic response, as evidenced by variations in search interest across CONUS. It is also apparent that the 2ml and 3ml models (which represents the 2 months and 3 months lagged input images) with R^2 values of 0.61 and 0.62 demonstrated the strongest relationships - pointing towards the existence of a lag between occurrences of MD and rise in people's SI.
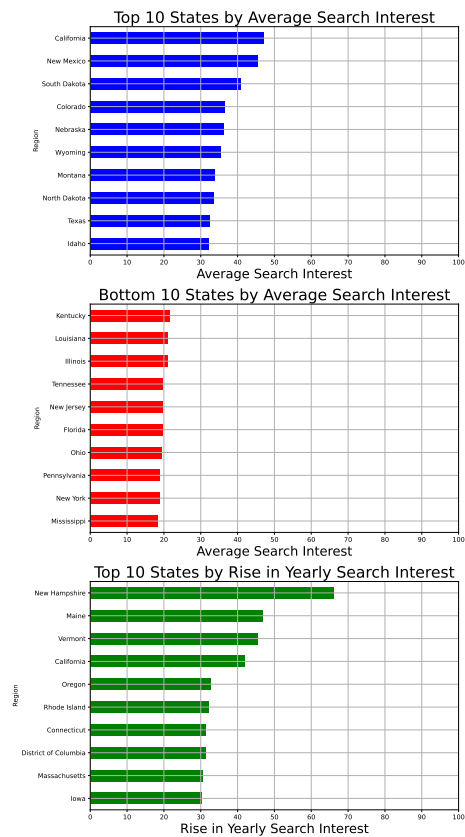

Figure 4: Results of the search interest analysis showing the top 10 and bottom 10 states in terms of the average search interest followed by the top 10 states by the rise in yearly search interest.

We generated a map of the best lag index (as explained in section 2.2)

17
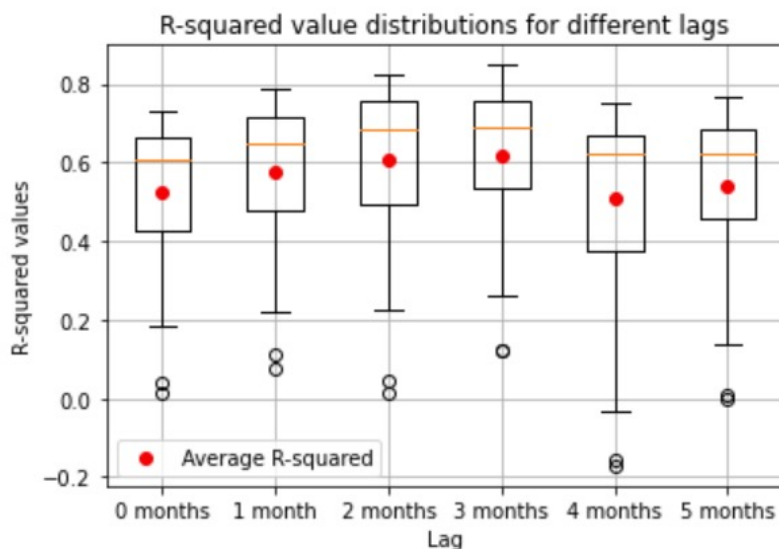
Figure 5: R^2 value distribution for different models - significant nonlinear correlations are found between MD occurrences and associated search interest across CONUS. The 2ml and 3ml models demonstrated the strongest relationships.

to obtain a snapshot of how the lag between occurrence of MD and rise in public SI in drought topics vary over CONUS (Fig. 6). We again observe that the 2ml and 3ml models (2 and 3 months lag) were the best performing lag models over CONUS. This indicates a clear existence of a lag variable which explains the delay between MD and rise in people's SI in drought topics in CONUS.

There are multiple factors which could drive a lag variable like this. We observe in Fig. 6 that regions with lag time less than or equal to 1 month generally rely on rain-fed irrigation (midwest and east coast) while states with lag times greater than or equal to 2 months mostly rely on water storage (surface reservoirs, aquifers) for irrigation. The types of crops grown and

18

water availability for irrigation (rain-fed or not) in these regions appear to be significant driving factors. Several studies have discussed the diverse impact of droughts and water scarcity on public reactions and opinions. For example, AghaKouchak et al. [24] argued that concurrent droughts and extreme heatwaves from climate change have significant social implications, and they could influence public opinions and reactions. Drier conditions are increasingly linked to public health issues [25, 26] and vegetation health as well [27, 28], which impact public perception of droughts and water availability, and subsequently, their interest in drought topics.
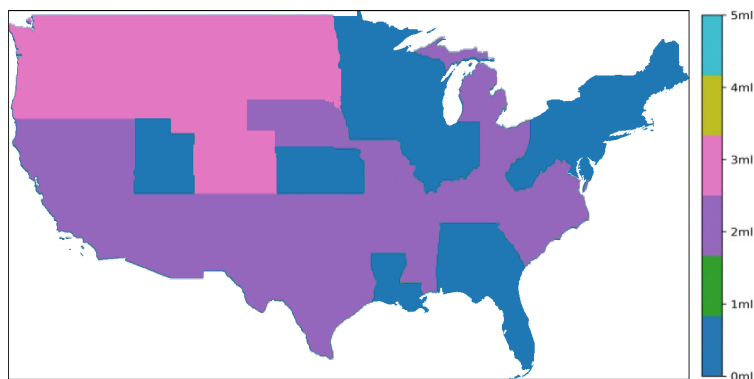
Figure 6: Distribution of best lag models over CONUS - 2ml and 3ml models (2 and 3 months lag) were the best performing models.

3.2. Does the relationship between MD occurrences and people's SI on drought topics demonstrate spatial variation across the CONUS?

We calculated the time series of U-Net outputs during the test period and tested the model performances for each individual pixel (Fig. 7). Our results

19

show explicit spatial variation of the relationship between MD and public SI on drought topics across CONUS.
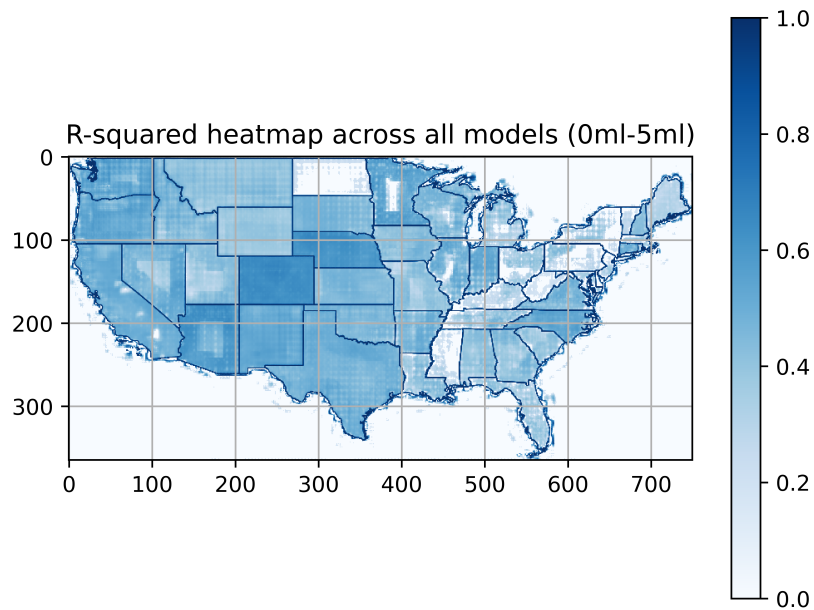

Figure 7: R^2 values averaged over the test period for CONUS and averaged across six models. Significant spatial variability can be seen in the relationship between MD and SI over CONUS.

State-level average test period R^2 values (across all the 6 models with different lags) are shown in Fig. 8. Colorado, South Carolina, New Jersey, and Nebraska had the highest average R^2 values, indicating that the SI of their residents have varied significantly with local drought conditions over our test period. On the other hand, CA, OR, NV, and ID had the lowest average R^2 values, showing that the SI of their residents have not varied significantly in drought topics with varying degrees of meteorological drought over our test period.

20

Colorado has been in the midst of droughts (starting from 2000, with severe drought affecting significant portion of the state between 2002-2004, 2012-2013, 2018-2019, 2020-2022)(droughtmonitor.unl.edu), and much of the state has experienced water scarcity fueled by depleting snowpack [29] and below average precipitation. South Carolina is also experiencing a drought, mostly in the Upstate and Midlands, but the conditions are not as severe as in Colorado. The drought in South Carolina has had an impact on agriculture [30], recreation, and the environment (http://www.scdrought.com/impacts.html). New Jersey has experienced abnormally dry conditions, but the state is not in a drought. However, these conditions are affecting the environment [31, 32, 30]. Nebraska has also experienced a moderate drought, with much of the state experiencing abnormally dry or drought conditions, adversely impacting agriculture and the environment [5, 33, 34]. The droughts in Colorado, South Carolina, New Jersey, and Nebraska are more recent compared to states like California, Oregon, and Nevada. The drought in California has been going on for over 20 years, while the drought trends in Colorado, South Carolina, Nebraska have been increasing [35]. In the initial periods of a prolonged drought, surface and groundwater reservoirs create a time buffer between meteorological and anthropogenic drought. Perhaps people become desensitized to drought topics after a certain period in a prolonged drought - this may explain why SI is more correlated to meteorological droughts in comparatively recently affected states during the model test period.
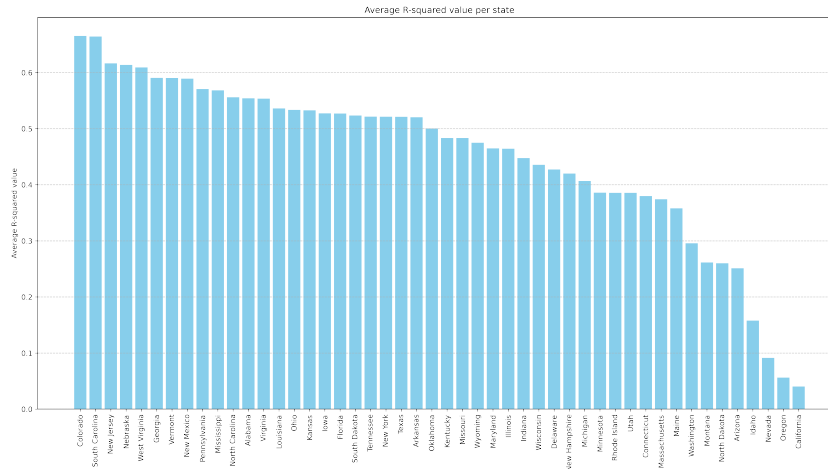
Figure 8: R^2 values (across the 6 models) for the relationship between MD and public SI in drought topics: Variation across the CONUS over the test period.

3.3. *Have people in MD hotspots become increasingly interested in drought topics?*

As described in section 2.2, we created a map to identify MD hotspots over CONUS between 2004-2020 (Fig. 9). We deem areas with average $SPEI$ below zero to be drought hotspots. From the generated map, it is apparent that parts of WA, OR, CA, NV, AZ, UT, ID, NE, ND, SD, MT, CO, NM, TX, OK, MS, KY, OH, GA, FL, NC, SC, TN, NJ and parts of their surrounding states have become drought hotspots.

To investigate relationships between worsening droughts (decreasing SPEI) and increasing public SI at a state level, we conducted trend analyses on the entire study period. We found significant negative correlation ($r = -0.28, p-value = 0.0001$) in trends between states with decreasing SPEI and
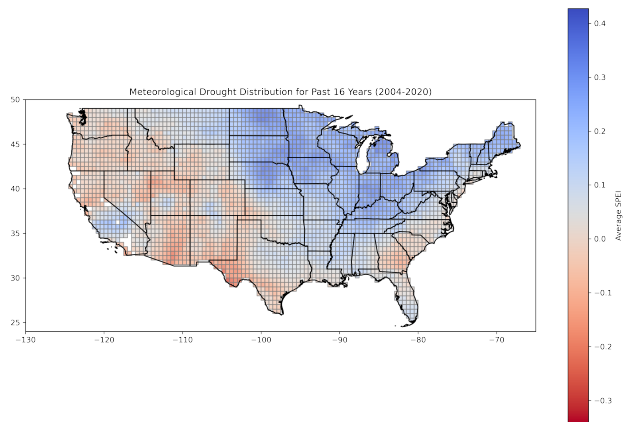
22

Figure 9: Drought hotspots in CONUS between 2004 and 2020.

increasing SI (Fig.10), indicating that people's search interest has generally risen with increasingly dry conditions in these states.

We further broke down the trend analysis into smaller time periods to look at hotspots and trends over shorter periods (Fig. 11). For the state of California, we found that even though SPEI demonstrated a downward trend over the three periods, people's SI has not trended upwards for the most recent time period (2016-2020) of our analysis.

These findings indicate that with worsening drought conditions in different CONUS states, public SI on drought topics also rose notably. Public SI trend in CA between 2016 and 2020 was not significant despite the drought conditions worsening over the previous 10 years. These observations warrant further insights into the underlying mechanisms driving these changes.
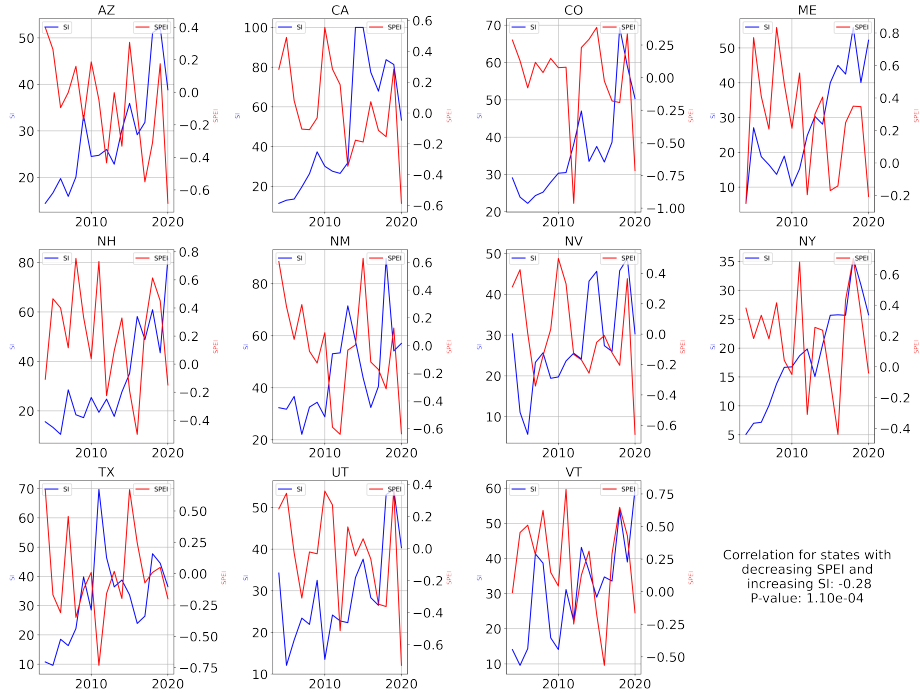
23

Figure 10: States with decreasing SPEI trends (left axis and red lines) and increasing SI trends (right axis and blue lines) between 2004 and 2020. Significant negative correlation ($r = -0.28, p - value = 0.0001$) was found between decreasing SPEI and increasing SI for these states.

3.4. Have people's reactions to drought become more polarized?

As previously discussed in section 2.2, we apply sentiment analysis on five million tweets (containing drought terms). These tweets were not geo-tagged and therefore a representative of the global twitter community. Upon observing the variability of public sentiment, we find that both positive sentiment($r = 0.24, p - value = 0.0018, BF10 = 12.36$) and negative sentiment ($r = 0.24, p - value = 0.0017, BF10 = 12.91$) tweets have slightly trended upwards between 2004 and 2020. On the contrary, the percentage of tweets with neutral sentiment have decreased ($r = -0.42, p - value =$
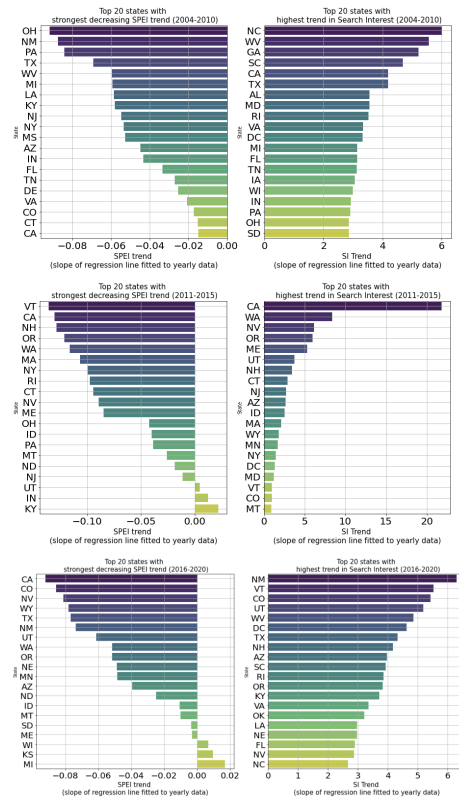
24

Figure 11: SPEI and SI trends by state (for top 20 states) broken down into three time periods: 2004-2010, 2011-2015, 2016-2020. For time period 2016-2020, people's SI CA has not trended upwards for California despite the SPEI trending downward for the state over all the periods.

$9.95e-09, BF10 = 1.21e+06$) in relation to the positive and negative tweets over the same period (Fig. 12).

Our findings suggest that the public sentiments towards droughts may be becoming more polarized. This is likely due to multiple factors which could include increasing severity of droughts, increasing politicization of climate change, increased regulations over groundwater to prevent groundwater overdraft, and spread of misinformation over the social media sphere. One

possible reason for these trends could be that as drought conditions worsen or become more prevalent, public awareness and concern grow, leading to more online searches and discussions about the topic. Positive sentiments could arise from discussions around successful drought management strategies, water conservation efforts, or community resilience. Negative sentiments might stem from the adverse impacts of droughts, such as crop loss, water shortages, and the associated socio-economic hardships. It can also be said that the rise in sentiment polarity is influenced by increasing public engagement with environmental issues more broadly. As discussions around specific environmental phenomena (like droughts) become increasingly popular, it is reasonable to think that they will become emotionally charged and polarized.
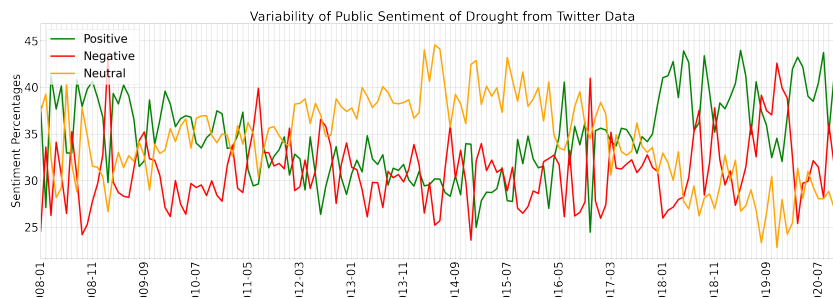

Figure 12: Variability of (global) public sentiment on drought topics in twitter and public search interest on droughts.Both positive sentiment and negative sentiment in tweets have slightly trended upwards between 2004 and 2020. On the contrary, the percentage of tweets with neutral sentiment have decreased

4. Conclusions & Discussion

We applied U-Net models to understand the relationships between MD and people's interest in drought topics over CONUS. To do this, we leveraged

26

$SPEI$, Google Trends SI, and Twitter data. The primary findings of this study are (see the four research questions outlined in Section 1.1):

- We found that people do respond to MD by searching Google for drought-related topics. We found that correlations between SPEI and SI were lagged at around 2 to 3 months with averaged R^2 values of SI predicted from SPEI of > 0.6.

- We found that relationships between MD and people's SI in drought terms vary over CONUS. We found the strongest relationships in Colorado, South Carolina, New Jersey and Nebraska.

- We identified MD hotspots in the CONUS and found that SI in drought topics have increased in states with worsening drought conditions. However, more recently (2016-2020), this effect was absent for California, which has the overall highest SI and has been experiencing droughts more or less consistently over the entire study period.

- Upon applying sentiment analysis to 5 million global drought-related tweets, we found that people's reactions to droughts may be becoming more polarized. This rise in polarity of emotions is happening alongside increasing global public SI in drought topics (from Google Trends).

Our findings strongly point towards a lagged non-linear entanglement between the occurrence of MD and rise in people's awareness on drought topics in the United States. Overall, public SI is notably higher and also increasing

27

in the regions with persistently dry or worsening drought conditions, except recently for California. These observations provide impetus for future studies investigating the underlying mechanisms driving human awareness of droughts. For example, do people search less about droughts with changing drought conditions as they become increasingly knowledgeable/aware over time? We also encourage future studies to focus on the explanation of the lag variable between occurrence of MD and rise relevant public SI - for example, exploring how meteorological droughts impact agricultural, hydrological, and socioeconomic droughts and quantifying the multidimensional non-stationary interplay between these phenomena and their corresponding human responses. The results of our study boosts the feasibility of training large-domain drought models in the sense that we provided the evidence towards potential end-users/stakeholders.

As the impacts of anthropogenic-driven climate change become increasingly felt and realized by humans across the world, we expect future experiments to find more complex relationships between extreme weather events (such as droughts) with people's engagement on different platforms across the global web. Given this scenario, computer vision models, such as our custom U-Nets, will continue to be significantly useful towards understanding (evolving) human-drought interactions.

5. Acknowledgements

References

[1] A. B. Smith, J. L. Matthews, Quantifying uncertainty and variable sensitivity within the us billion-dollar weather and climate disaster cost estimates, Natural Hazards 77 (2015) 1829–1851.

[2] H. E. Campbell, R. M. Johnson, E. H. Larson, Prices, devices, people, or rules: the relative effectiveness of policy instruments in water conservation 1, Review of policy research 21 (2004) 637–662.

[3] J. M. Clarke, R. R. Brown, Understanding the factors that influence domestic water consumption within melbourne, Australasian Journal of Water Resources 10 (2006) 261–268.

[4] D. C. Adams, D. Allen, T. Borisova, D. E. Boellstorff, M. D. Smolen, R. L. Mahler, The influence of water attitudes, perceptions, and learning preferences on water-conserving actions, Natural Sciences Education 42 (2013) 114–122.

[5] D. L. Woudenberg, D. A. Wilhite, M. J. Hayes, Perception of drought hazard and its sociological impacts in south-central nebraska, Great Plains Research (2008) 93–102.

[6] J. Urquijo, L. De Stefano, Perception of drought and local responses by farmers: a perspective from the jucar river basin, spain, Water Resources Management 30 (2016) 577–591.

[7] Y. Bahta, A. Jordaan, F. Muyambo, Communal farmers' perception of drought in south africa: Policy implication for drought risk reduction, International Journal of Disaster Risk Reduction 20 (2016) 39–50.

[8] D. M. Gholson, D. E. Boellstorff, S. R. Cummings, K. L. Wagner, M. C. Dozier, A survey of public perceptions and attitudes about water availability following exceptional drought in texas, Journal of Contemporary Water Research & Education 166 (2019) 1–11.

[9] W. Shao, J. Kam, E. Cass, Public awareness and perceptions of drought: A case study of two cities of alabama, Risk, Hazards & Crisis in Public Policy (2022).

[10] S. McLafferty, Conducting questionnaire surveys, Key methods in geography 3 (2016) 129–142.

[11] J. J. Vaske, Advantages and disadvantages of internet surveys: Introduction to the special issue, Human Dimensions of Wildlife 16 (2011) 149–153.

[12] R. J. Fisher, Social desirability bias and the validity of indirect questioning, Journal of consumer research 20 (1993) 303–315.

[13] R. M. Groves, Nonresponse rates and nonresponse bias in household surveys, Public opinion quarterly 70 (2006) 646–675.

[14] M. Martin, et al., Computer and internet use in the united states: 2018, American Community Survey Reports. Recuperado de https://www. census. gov/library/publications/2021/acs/acs-49. html (2021).

[15] T. Carneiro, R. V. M. Da Nóbrega, T. Nepomuceno, G.-B. Bian, V. H. C. De Albuquerque, P. P. Reboucas Filho, Performance analysis of google colaboratory as a tool for accelerating deep learning applications, IEEE Access 6 (2018) 61677–61685.

[16] A. C. Yang, N. E. Huang, C.-K. Peng, S.-J. Tsai, Do seasons have an influence on the incidence of depression? the use of an internet search engine query data as a proxy of human affect, PloS one 5 (2010) e13728.

[17] S. Stephens-Davidowitz, The cost of racial animus on a black candidate: Evidence using google search data,

Journal of Public Economics 118 (2014) 26–40. URL: https://www.sciencedirect.com/science/article/pii/S0047272714000929. doi:https://doi.org/10.1016/j.jpubeco.2014.04.010.

[18] Y. Hong, J. Lawrence, D. Williams, I. Mainous, Population-level interest and telehealth capacity of us hospitals in response to covid-19: cross-sectional analysis of google search and national hospital survey data. jmir public health surveill. 2020 apr 07; 6 (2): e18961. doi: 10.2196/18961, ????

[19] V. S. Arora, M. McKee, D. Stuckler, Google trends: Opportunities and limitations in health and health policy research, Health Policy 123 (2019) 338–341.

[20] J. Mellon, Where and when can we use google trends to measure issue salience?, PS: Political Science & Politics 46 (2013) 280–290.

[21] S. Beguería, sbeguería/speibase: Version 2.7, 2022. URL: https://doi.org/10.5281/zenodo.5864391. doi:10.5281/zenodo.5864391.

[22] O. Ronneberger, P. Fischer, T. Brox, U-net: Convolutional networks for biomedical image segmentation, in: Medical Image Computing and Computer-Assisted Intervention–MICCAI 2015: 18th International Conference, Munich, Germany, October 5-9, 2015, Proceedings, Part III 18, Springer, 2015, pp. 234–241.

[23] C. Hutto, E. Gilbert, Vader: A parsimonious rule-based model for senti-
ment analysis of social media text, in: Proceedings of the international
AAAI conference on web and social media, volume 8, 2014, pp. 216–225.

[24] A. AghaKouchak, L. Cheng, O. Mazdiyasni, A. Farahmand, Global
warming and changes in risk of concurrent climate extremes: Insights
from the 2014 california drought, Geophysical Research Letters 41
(2014) 8847–8852.

[25] R. Barrera, V. Acevedo, M. Amador, M. Marzan, L. E. Adams, G. Paz-
Bailey, El niño southern oscillation (enso) effects on local weather, ar-
boviral diseases, and dynamics of managed and unmanaged populations
of aedes aegypti (diptera: Culicidae) in puerto rico, Journal of Medical
Entomology (2023) tjad053.

[26] E. Moyo, L. G. Nhari, P. Moyo, G. Murewanhema, T. Dzinamarira,
Health effects of climate change in africa: A call for an improved imple-
mentation of prevention measures, Eco-Environment & Health (2023).

[27] A. R. Chilakala, P. Pandey, A. Durgadevi, M. Kandpal, B. S. Patil,
K. Rangappa, P. C. O. Reddy, V. Ramegowda, M. Senthil-Kumar,
Drought attenuates plant responses to multiple rhizospheric pathogens:
A study on a dry root rot-associated disease complex in chickpea fields,
Field Crops Research 298 (2023) 108965.

[28] L. Bao, L. Yu, Y. Li, F. Yan, V. Lyne, C. Ren, Climate change impacts

on agroecosystems in china: Processes, mechanisms and prospects, Chinese Geographical Science (2023) 1–18.

[29] A. J. Heldmyer, N. R. Bjarke, B. Livneh, A 21st-century perspective on snow drought in the upper colorado river basin, JAWRA Journal of the American Water Resources Association (2023).

[30] M. Noel, D. Bathke, B. Fuchs, D. Gutzmer, T. Haigh, M. Hayes, M. Poděbradská, C. Shield, K. Smith, M. Svoboda, Linking drought impacts to drought severity at the state level, Bulletin of the American Meteorological Society 101 (2020) E1312–E1321.

[31] R. Mohammed, L. Maskal, Drought climatology and impacts in the northeast: Case studies for new jersey and delaware, in: AGU Fall Meeting Abstracts, volume 2021, 2021, pp. NH15F–0501.

[32] B. Johnson, M. Sukhdeo, Drought-induced amplification of local and regional west nile virus infection rates in new jersey, Journal of medical entomology 50 (2013) 195–204.

[33] A. M. Abadi, Y. Gwon, M. O. Gribble, J. D. Berman, R. Bilotta, M. Hobbins, J. E. Bell, Drought and all-cause mortality in nebraska from 1980 to 2014: Time-series analyses by age, sex, race, urbanicity and drought severity, Science of the Total Environment 840 (2022) 156660.

[34] P. Nasta, J. B. Gates, Plot-scale modeling of soil water dynamics and impacts of drought conditions beneath rainfed maize in eastern nebraska, Agricultural water management 128 (2013) 120–130.

[35] D. L. Ficklin, J. T. Maxwell, S. L. Letsinger, H. Gholizadeh, A climatic deconstruction of recent drought trends in the united states, Environmental Research Letters 10 (2015) 044009.

[36] S. Minaee, Y. Boykov, F. Porikli, A. Plaza, N. Kehtarnavaz, D. Terzopoulos, Image segmentation using deep learning: A survey, IEEE transactions on pattern analysis and machine intelligence 44 (2021) 3523–3542.

[37] D. Qin, J. Yu, G. Zou, R. Yong, Q. Zhao, B. Zhang, A novel combined prediction scheme based on cnn and lstm for urban pm 2.5 concentration, IEEE Access 7 (2019) 20050–20059.

[38] H. Hasan, H. Z. Shafri, M. Habshi, A comparison between support vector machine (svm) and convolutional neural network (cnn) models for hyperspectral image classification, in: IOP Conference Series: Earth and Environmental Science, volume 357, IOP Publishing, 2019, p. 012035.

[39] D. Zeng, S. Zhang, F. Chen, Y. Wang, Multi-scale cnn based garbage detection of airborne hyperspectral data, IEEE Access 7 (2019) 104514–104527.

[40] R. Barzegar, M. T. Aalami, J. Adamowski, Coupling a hybrid cnn-lstm deep learning model with a boundary corrected maximal overlap discrete wavelet transform for multiscale lake water level forecasting, Journal of Hydrology 598 (2021) 126196.

[41] M. Panahi, N. Sadhasivam, H. R. Pourghasemi, F. Rezaie, S. Lee, Spatial prediction of groundwater potential mapping based on convolutional neural network (cnn) and support vector regression (svr), Journal of Hydrology 588 (2020) 125033.

[42] X. Guo-yan, Z. Jin, S. Cun-you, H. Wen-bin, L. Fan, Combined hydrological time series forecasting model based on cnn and mc, Computer and Modernization (2019) 23.

[43] D. Hussain, T. Hussain, A. A. Khan, S. A. A. Naqvi, A. Jamil, A deep learning approach for hydrological time-series prediction: A case study of gilgit river basin, Earth Science Informatics 13 (2020) 915–927.

[44] T. Tu, K. Ishida, A. Ercan, M. Kiyama, M. Amagasaki, T. Zhao, Hybrid precipitation downscaling over coastal watersheds in japan using wrf and cnn, Journal of Hydrology: Regional Studies 37 (2021) 100921.

[45] F. R. Adaryani, S. J. Mousavi, F. Jafari, Short-term rainfall forecasting using machine learning-based approaches of pso-svr, lstm and cnn, Journal of Hydrology 614 (2022) 128463.

[46] Y. Wang, Z. Fang, H. Hong, L. Peng, Flood susceptibility mapping using convolutional neural network frameworks, Journal of Hydrology 582 (2020) 124482.

[47] C. M. Song, Data construction methodology for convolution neural network based daily runoff prediction and assessment of its applicability, Journal of Hydrology 605 (2022) 127324.

[48] Y. Li, W. Wang, G. Wang, Q. Tan, Actual evapotranspiration estimation over the tuojiang river basin based on a hybrid cnn-rf model, Journal of Hydrology 610 (2022) 127788.

[49] S. Kabir, S. Patidar, X. Xia, Q. Liang, J. Neal, G. Pender, A deep convolutional neural network model for rapid prediction of fluvial flood inundation, Journal of Hydrology 590 (2020) 125481.

Appendix A. The U-Net Model

Computer vision techniques such as image segmentation has surged in popularity in recent years, with applications in scene understanding, medical image analysis, robotic perception, video surveillance, augmented reality, and image compression among others [36]. Deep learning models such as Convolutional Neural Networks (CNN) are being increasingly applied in environmental sciences, e.g., air quality modeling [37], image classification [38, 39] etc. In hydrological sciences, CNNs have been used for lake water level

37

forecasting [40], prediction of groundwater potential mapping [41], hydrological time series forecasting modeling [42, 43], rainfall forecasting [44, 45], flood susceptibility mapping [46], daily runoff prediction [47], evapotranspiration estimation [48], and rapid production of fluvial flood inundation [49] among other applications. In this study, we approach understanding human-meteorological drought(MD)interactions using large-scale (CONUS scale) maps/images, making CNNs ideal candidates for our objectives. We used U-Net, which is a deep learning model used that was developed for image segmentation to learn relationships between meteorological droughts and search interest. Inputs to the model are SPEI maps over the CONUS and targets are Google SI maps over the CONUS.

Appendix A.1. Model Architecture

The U-Net is a convolutional neural network with an encoder-decoder architecture. Our model architecture (Fig. A.13) has two encoder blocks. Each encoder block has two convolutional layers followed by ReLU activation functions and one Max-pooling layer. The first encoder block captures low-level features of the input images, e.g. edges, corners and textures. The second encoder block builds on the first one by capturing higher level features and patterns. A middle block consisting of two convolutional layers and ReLU activation functions processes the high-level features captured by the encoder blocks. There are two decoder blocks - the first one starts the upsampling process to generate the output image. It consists of a transposed

convolutional layer (also called deconvolutional layer) followed by two convolutional layers and corresponding ReLU activation layers. The first decoder block combines the features from the middle block with the high level features of the second encoder block. The second decoder block continues the upsampling process by combining the features from the first decoder block with the low-level features from the first encoder block. It has one transposed convolutional layer followed by two 3x3 convolutional layers and one 1x1 convolutional layer to produce the final output image. In a broad sense, this allows the model to skip connections, allowing information to flow directly from the encoder to the decoder blocks, helping the network preserve finer features in the output image.
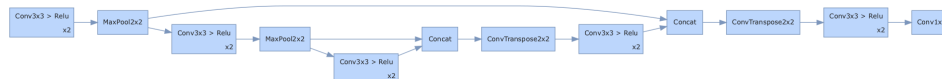

Figure A.13: Our custom U-Net Model Architecture (image generated with Hiddenlayer library).

Appendix A.2. Model Training

We split our training and testing data using an 80/20 ratio, so that 163 months of SPEI data and corresponding SI data were used for training and 41 months of data were used for testing. We trained six U-Net models on the six different sets of SPEI images (as defined earlier). Starting from zero months lag (0ml) to 5 months lag (5ml). These lags allow us to statistically explore any temporal trends between meteorological drought events and an-

thropogenic response to these events (in terms of when people within our study domain become interested in topics related to droughts). The training process involved feeding input SPEI images and their corresponding SI labels to the model and loss function, respectively. We used an adaptive moment (ADAM) optimizer with a Mean Squared Error (MSE) loss, a batch size of 1 image, and 20 training epochs.

Appendix A.3. Model Evaluation

We evaluated models on the test set of 41 images. The output of the U-Net models are probability maps that have the same shape as the input image (i.e., the same spatial resolution as the SPEI images). These vectors represent the probability of each pixel belonging to the target class (SI maps). We then calculated the average R-squared scores for each model.